Supplementary Material

Intelligent phase-transition MnO_2 single-crystal shell enabling high-capacity Li-rich layered cathode in Li-ion batteries

Deyuan Liu, Jian Yang, Junming Hou, Jiaxuan Liao, Mengqiang Wu*

School of Materials and Energy, University of Electronic Science and Technology of China, 2006 Xiyuan Ave, West High-Tech Zone, Chengdu, 611731, P. R. China

* Corresponding author. E-mail: *mwu@uestc.edu.cn* (Mengqiang Wu)

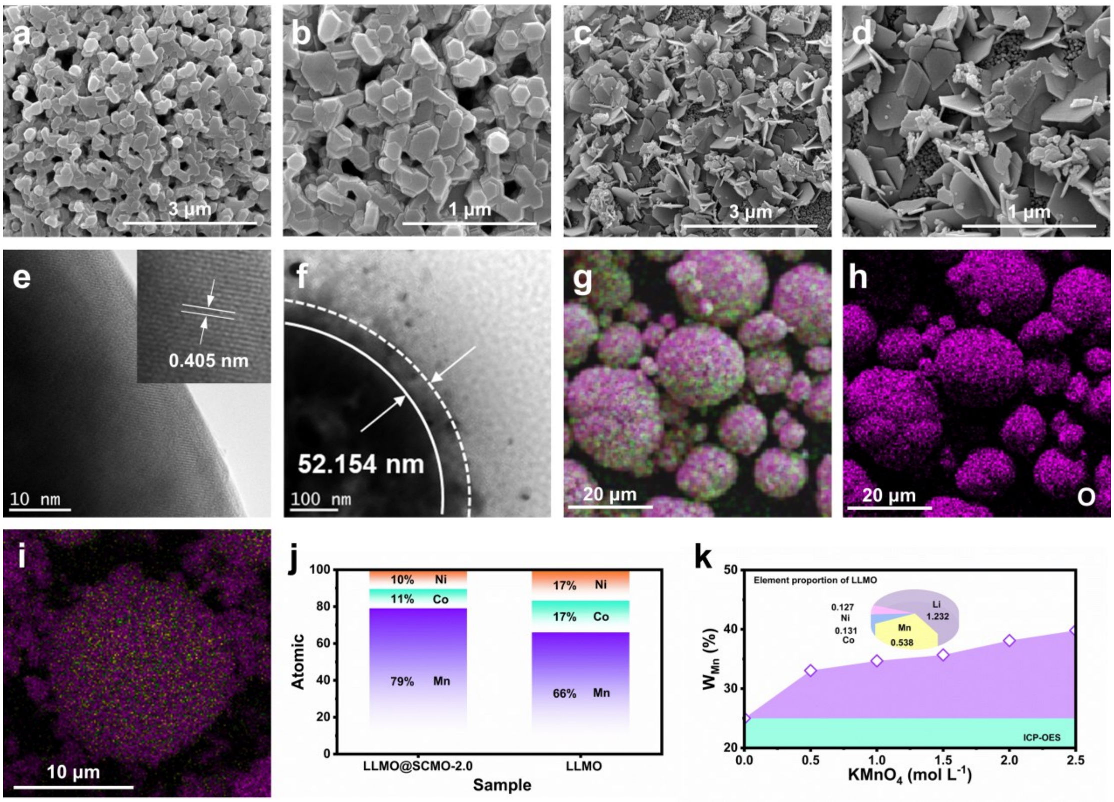

Figure S1. (a-b, c-d) SEM images of LLMO and SCMO@LLMO-2.0, (e) HRTEM image of LLMO, (f) TEM images of SCMO@LLMO-2.0, (g, h) EDS mapping images of LLMO, (i) SCMO@LLMO-2.0, (j) EDS Atomic (%) of SCMO@LLMO-2.0 and LLMO, (k) ICP-OES element proportion of LLMO and W_{Mn} (%) of SCMO@LLMOs.

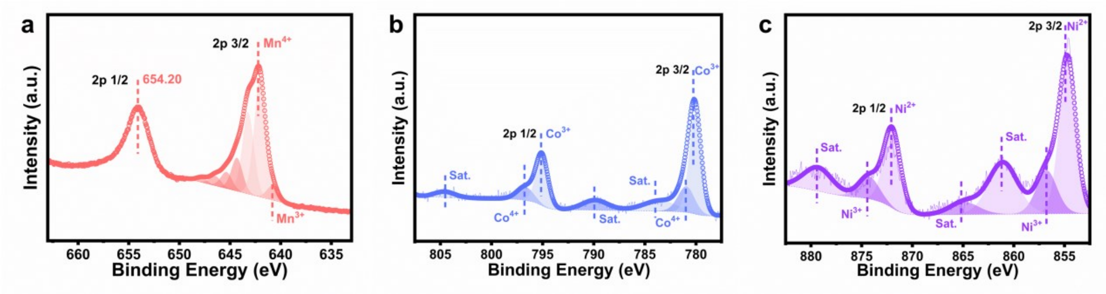

Figure S2. (a-c) The X-ray photoelectron spectroscopy (Mn, Co and Ni) of LLMO.

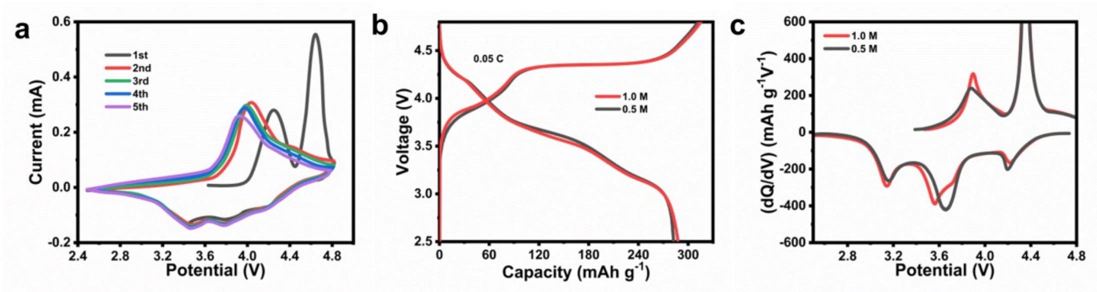

Figure S3. (a) The CV curve of LLMO, (b) The initial charge and discharge curves of SCMO@LLMOs, (c) The capacity differential curve of (b).

‘

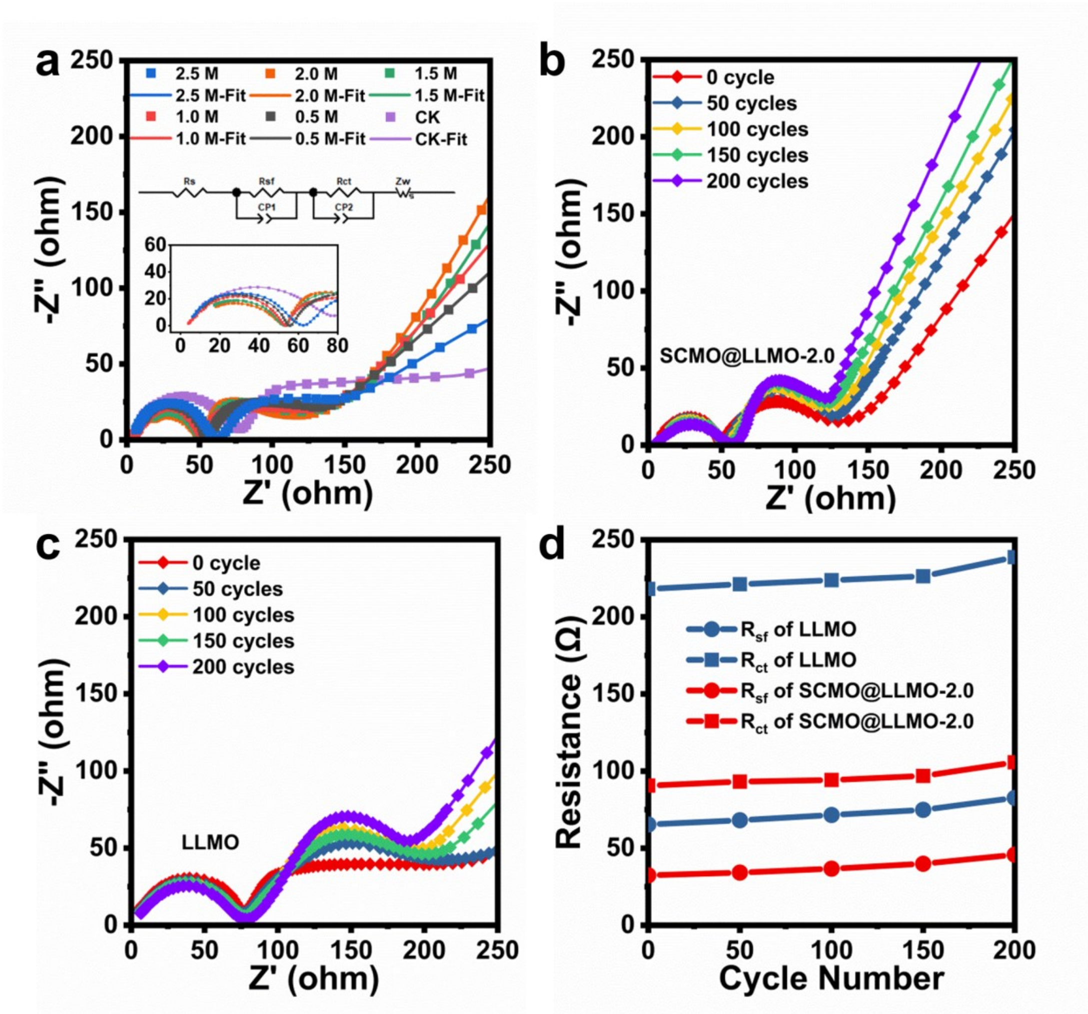

Figure S4. (a) Nyquist plots of the SCMO@LLMOs before cycling, (b, c) Nyquist plots of SCMO@LLMO-2.0 and LLMO of 0, 50, 100, 150, and 200 cycles, respectively. (d) The R_{sf} and R_{ct} of LLMO and SCMO@LLMO-2.0 of 0, 50, 100, 150, and 200 cycles, respectively.

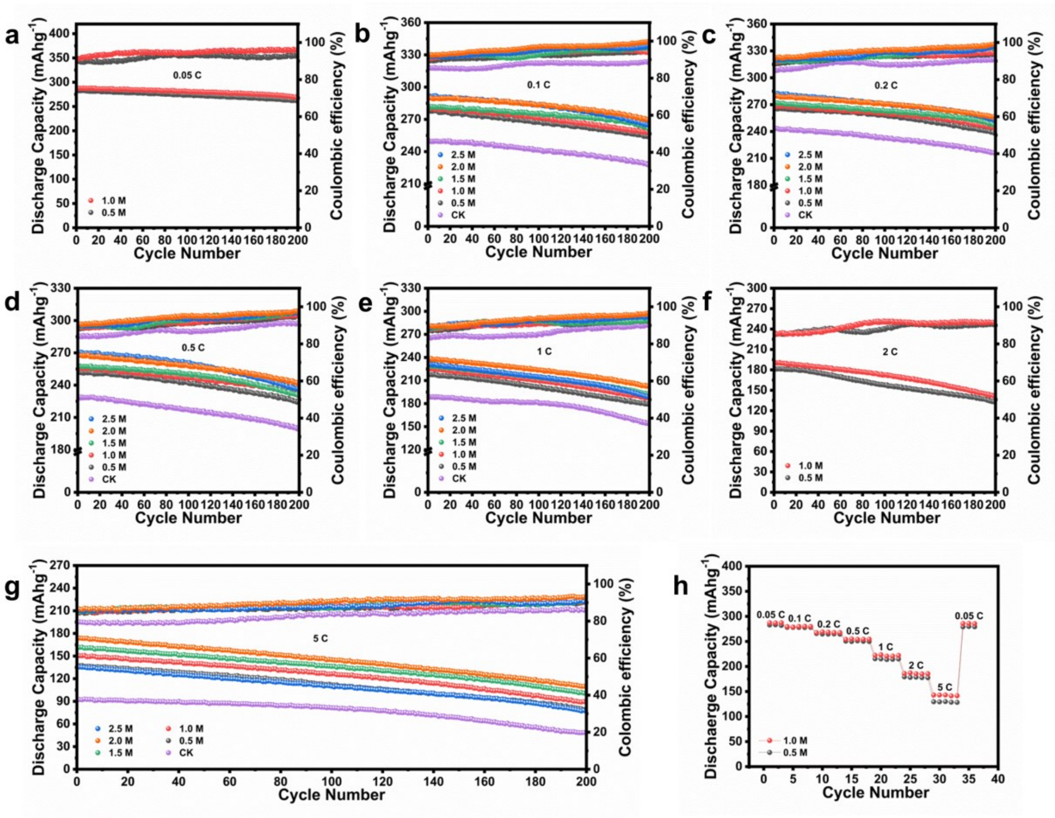

Figure S5. (a-g) The cycling performance curves of SCMO@LLMOs under current densities of 0.05 C, 0.1 C, 0.2 C, 0.5 C, 1 C ,2 C, and 5 C, respectively, (h) The rate performance curves of SCMO@LLMOs under current densities of 0.05 C, 0.1 C, 0.2 C, 0.5 C, 1 C ,2 C, and 5 C, respectively.

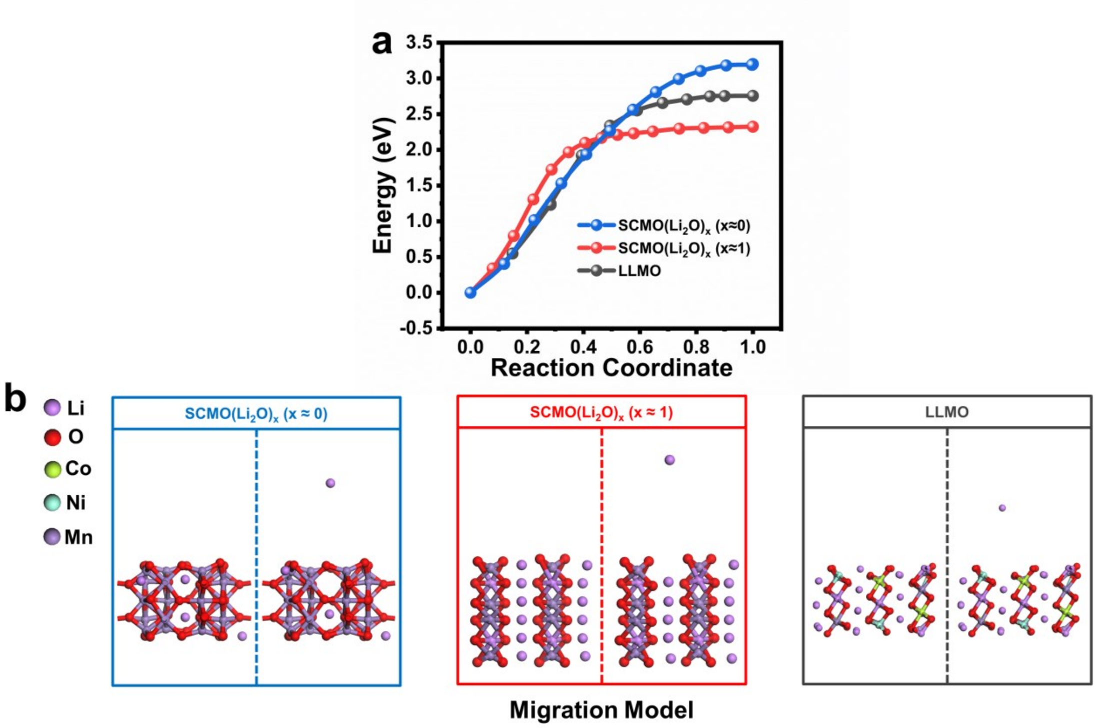

Figure S6. The (a) diffusion paths and (b) migration models of LLMO, SCMO(Li_2O)$_x$ ($x \approx 0$), and SCMO(Li_2O)$_x$ ($x \approx 1$), respectively.

Table S1. Comparison with similar modifications of LLMO.

Modification	Current density (C)	Initial coulombic efficiency (%)	Initial discharge capacity (mAh g^{-1})	Cycle number (#)	Capacity retention ratio (%)
SCMO shell (This paper)	0.05	93.0	296.9	100/200	97.9/93.9
	0.1	92.6	289.8	100/200	97.8/92.8
	0.2	91.8	279.3	100/200	96.9/91.6
	0.5	90.5	267.8	100/200	96.3/90.2
PB coating[1]	0.1	85.7	281.7	100	77.2
Injection of V-O[2]	0.1	79.6	221.9	300	92.6
Mg doping[3]	0.1	78.5	273.0	100	80.6
Al doping[4]	0.1	77.3	255.0	100	96.0
Ni substitution [5]	0.2	70.6	242.9	150	95.0
Li_2TiO_3 coating[6]	0.1	78.6	218.0	50	77.5
$AlPO_4$ coating[7]	0.2	78.9	267.2	50	73.4
Fluorine doping[8]	0.2	68.1	220.0	100	79.7
Cr Doping[9]	0.2	97.7	219.0	133	77.6
Carbon coating[10]	0.2	96.7	263.0	100	70
Graphene oxide[11]	0.2	87.3 (0.05 C)	238	50	79.4
MgO coating[12]	1	78.0 (0.1 C)	260.8 (0.1 C)	100	96.4
Na-stablization[13]	0.1	87.5	307.0	100 (0.3 C)	89.0 (0.3 C)
Ru substitution[14]	0.05	81.4	279.3	50 (0.2 C)	81.5 (0.2 C)
AlF_3 coating[15]	0.2	89.5	246.0	50	93.2
Al_2O_3 coating[16]	0.05	85.0	275.0	-	-
Al substitution[17]	0.1	92.9	262.0	-	-
$LiFePO_4$ blending[18]	0.3	79.4	230.0	50	102.6
Double-layer coating[19]	0.05	98.0	298.0	30	89.7
V_2O_5 composite[20]	0.05	123.9	300	25	58.3

Table S2. The chemical reaction of synthesis process.

Stage	Chemical Reaction
Acid-tearment	H_2SO_4+$Mn(OH)_2$→$MnSO_4$+H_2O
Hydrotherm	$MnSO_4$+$KMnO_4$+H_2O→MnO_2+K_2SO_4+H_2SO_4
Calcining	$Mn(OH)_2$→MnO_2+H_2O

Table S3. The specific surface area (BET) and the pore size distribution ratio of SCMO@LLMO-2.0 and LLMO.

Sample	**Specific Surface Area (P/Po=0.2)**	**Pore Size Distribution Ratio**		
		1-5 nm	**5-10 nm**	**＞10 nm**
SCMO@LLMO-2.0	96.475 m^2 g^{-1}	96.2%	3.7%	0.1%
		1-5 nm	**5-10 nm**	**＞10 nm**
LLMO	75.227 m^2 g^{-1}	89.6%	10.3%	0.1%

Table S4. Comparison of XRD Rietveld refinement data of SCMO@LLMO-2.0 and LLMO.

Sample	Phase	Lattice parameters（Å）	Atomic occupancy and position: Li	Mn	Ni	Co	Proportion (%)	c/a	Ni[3b]/Li[3b]
SCMO@LLMO-2.0	**C/2m**	a=4.955772 b=8.552964 c=5.020708 β=109.3154	1.0000[2b][2b][4h]	1.0000[4g]			92.402	5.002496091	0
	R-3m	a=b=2.868085 c=14.347584	[3b]1.0000	0.5912[3a]	[3a]0.1155	0.2360[3a]	7.598		
LLMO	**C/2m**	a=4.941426 b=8.549039 c=5.024958 β=109.2163	1.0000[2b][2b][4h]	1.0000[4g]			90.528	5.034466955	0.035554
	R-3m	a=b=2.853922 c=14.367976	[3b]0.8691 [3a]0.0309	0.5764[3a]	[3a]0.1140 [3b]0.0309	0.2320[3a]	9.472		

Table S5. XPS peak fitting data of SCMO@LLMO-2.0 and LLMO.

Sample	Ni	Co	Mn
SCMO@LLMO-2.0	（70.87%Ni^{2+}/29.13%Ni^{3+}）	（58.52%Co^{3+}/41.48%Co^{2+}）	（96.18%Mn^{4+}/3.82%Mn^{3+}）
	2p3/2 854.76Ni^{2+}	2p3/2 780.14Co^{3+}	2p3/2 640.6Mn^{3+}
	856.53Ni^{3+}	780.74Co^{2+}	641.90Mn^{4+}; 642.93Mn^{4+};
	2p1/2 872.18Ni^{2+}	2p1/2 795.09Co^{3+}	643.59Mn^{4+}; 644.21Mn^{4+};
	874.32Ni^{3+}	796.48Co^{2+}	645.04Mn^{4+}; 646.16Mn^{4+}.
LLMO	（73.88%Ni^{2+}/26.13%Ni^{3+}）	（73.05%Co^{3+}/26.95%Co^{2+}）	（95.14%Mn^{4+}/4.86%Mn^{3+}）
	2p3/2 854.7Ni^{2+}	2p3/2 780.09Co^{3+}	2p3/2 640.85Mn^{3+}
	856.75Ni^{3+}	780.94Co^{2+}	642.06Mn^{4+}; 643.21Mn^{4+};
	2p1/2 871.99Ni^{2+}	2p1/2 795.07Co^{3+}	644.32Mn^{4+}; 645.35Mn^{4+};
	874.26Ni^{3+}	796.68Co^{2+}	646.45Mn^{4+}; 647.79Mn^{4+}.

Table S6. Electrochemical impedance fitting data of SCMO@LLMOs.

Sample	**R_s/Ω**	**R_{sf}/Ω**	**R_{ct}/Ω**	**σ_w**	**$D_{Li^+}/(cm^2 \cdot s^{-1}) *10^{-16}$**
Untreated	3.23	71.50	223.79	22.17	0.63806548996366
0.5 M	4.82	48.25	124.70	14.54	1.48863575650532
1.0 M	6.37	44.05	117.21	12.76	1.91081840722379
1.5 M	7.75	40.97	106.49	11.82	2.27621075223101
2.0 M	9.31	36.74	94.24	9.94	3.19335395775053
2.5 M	4.19	53.11	139.35	13.57	1.70797489965782

Reference

[1] Z. Xu, L. Ci, Y. Yuan, X. Nie, J. Li, J. Cheng, Q. Sun, Y. Zhang, G. Han, G. Min, J. Lu, Potassium Prussian blue-coated Li-rich cathode with enhanced lithium ion storage property, Nano Energy 75 (2020) 104942. https://doi.org/10.1016/j.nanoen.2020.104942.

[2] P. Yan, J. Zheng, Z.K. Tang, A. Devaraj, G. Chen, K. Amine, J.G. Zhang, L.M. Liu, C. Wang, Injection of oxygen vacancies in the bulk lattice of layered cathodes, Nat. Nanotechnol. 14 (2019) 602–608. https://doi.org/10.1038/s41565-019-0428-8.

[3] P.K. Nayak, J. Grinblat, E. Levi, M. Levi, B. Markovsky, D. Aurbach, Understanding the influence of Mg doping for the stabilization of capacity and higher discharge voltage of Li- and Mn-rich cathodes for Li-ion batteries, Phys. Chem. Chem. Phys. 19 (2017) 6142–6152. https://doi.org/10.1039/C6CP07383B.

[4] P.K. Nayak, J. Grinblat, M. Levi, E. Levi, S. Kim, J.W. Choi, D. Aurbach, Al doping for mitigating the capacity fading and voltage decay of layered Li and Mn-rich cathodes for Li-ion batteries, Adv. Energy Mater. 6 (2016) 114639849. https://doi.org/10.1002/aenm.201502398.

[5] P. Kumar Nayak, J. Grinblat, E. Levi, T.R. Penki, M. Levi, Y.K. Sun, B. Markovsky, D. Aurbach, Remarkably improved electrochemical performance of Li- and Mn-Rich cathodes upon substitution of Mn with Ni, ACS Appl. Mater. Inter. 9 (2017) 4309–4319. https://doi.org/10.1021/acsami.6b07959.

[6] E. Zhao, X. Liu, Z. Hu, L. Sun, X. Xiao, Facile synthesis and enhanced electrochemical performances of Li_2TiO_3-coated lithium-rich layered $Li_{1.13}Ni_{0.30}Mn_{0.57}O_2$ cathode materials for lithium-ion batteries, J. Power Sour. 294 (2015) 141–149. https://doi.org/10.1016/j.jpowsour.2015.06.059.

[7] F. Wu, X. Zhang, T. Zhao, L. Li, M. Xie, R. Chen, Multifunctional $AlPO_4$ coating for improving electrochemical properties of low-cost $Li[Li_{0.2}Fe_{0.1}Ni_{0.15}Mn_{0.55}]O_2$ cathode materials for lithium-ion batteries, ACS Appl. Mater. Inter. 7 (2015) 3773–3781. https://doi.org/10.1021/am508579r.

[8] L. Li, B.H. Song, Y.L. Chang, H. Xia, J.R. Yang, K.S. Lee, L. Lu, Retarded phase transition by fluorine doping in Li-rich layered $Li_{1.2}Mn_{0.54}Ni_{0.13}Co_{0.13}O_2$ cathode material, J. Power Sour. 283 (2015) 162–170. https://doi.org/10.1016/j.jpowsour.2015.02.085.

[9] B. Song, C. Zhou, H. Wang, H. Liu, Z. Liu, M.O. Lai, L. Lu, Advances in sustain stable voltage of Cr-Doped Li-Rich layered cathodes for lithium ion batteries, J. Electrochem. Soc. 161 (2014) A1723–A1730. https://doi.org/10.1149/2.0461410jes.

[10] B. Song, C. Zhou, Y. Chen, Z. Liu, M.O. Lai, J. Xue, L. Lu, Role of carbon coating in improving electrochemical performance of Li-rich $Li(Li_{0.2}Mn_{0.54}Ni_{0.13}Co_{0.13})O_2$ cathode, RSC Adv. 4 (2014) 44244–44252. https://doi.org/10.1039/C4RA04976D.

[11] B. Song, M.O. Lai, Z. Liu, H. Liu, L. Lu, Graphene-based surface modification on layered Li-rich cathode for high-performance Li-ion batteries, J. Mater.Chem. A 1 (2013) 9954–9965. https://doi.org/10.1039/C3TA11580A.

[12] S.J. Shi, J.P. Tu, Y.Y. Tang, X.Y. Liu, Y.Q. Zhang, X.L. Wang, C.D. Gu, Enhanced cycling stability of $Li[Li_{0.2}Mn_{0.54}Ni_{0.13}Co_{0.13}]O_2$ by surface modification of MgO with melting impregnation method, Electrochim. Acta 88 (2013) 671–679. https://doi.org/10.1016/j.electacta.2012.10.111.

[13] W. He, D. Yuan, J. Qian, X. Ai, H. Yang, Y. Cao, Enhanced high-rate capability and cycling stability of Na-stabilized layered $Li_{1.2}[Co_{0.13}Ni_{0.13}Mn_{0.54}]O_2$ cathode material, J. Mater.Chem. A 1 (2013) 11397. https://doi.org/10.1039/C3TA12296D.

[14] B. Song, M.O. Lai, L. Lu, Influence of Ru substitution on Li-rich $0.55Li_2MnO_3{\cdot}0.45LiNi_{1/3}Co_{1/3}Mn_{1/3}O_2$ cathode for Li-ion batteries, Electrochim. Acta 80 (2012) 187–195. https://doi.org/10.1016/j.electacta.2012.06.118.

[15] G.R. Li, X. Feng, Y. Ding, S.H. Ye, X.P. Gao, AlF_3-coated $Li(Li_{0.17}Ni_{0.25}Mn_{0.58})O_2$ as cathode material for Li-ion batteries, Electrochim. Acta 78 (2012) 308–315. https://doi.org/10.1016/j.electacta.2012.05.142.

[16] W.C. West, J. Soler, M.C. Smart, B.V. Ratnakumar, S. Firdosy, V. Ravi, M.S. Anderson, J. Hrbacek, E.S. Lee, A. Manthiram, Electrochemical behavior of layered solid solution $Li_2MnO_3-LiMO_2$ (M = Ni, Mn, Co) Li-Ion cathodes with and without alumina coatings, J. Electrochem. Soc. 158 (2011) A883. https://doi.org/10.1149/1.3597319.

[17] Z. Li, N.A. Chernova, J. Feng, S. Upreti, F. Omenya, M.S. Whittingham, Stability and rate capability of al substituted lithium-rich high-manganese content oxide materials for li-ion batteries, J. Electrochem. Soc. 159 (2012) A116–A120. https://doi.org/10.1149/2.044202jes.

[18] K.G. Gallagher, S.H. Kang, S.U. Park, S.Y. Han, $xLi_2MnO_3{\cdot}(1-x)LiMO_2$ blended with $LiFePO_4$ to achieve high energy density and pulse power capability, J. Power Sour. 196 (2011) 9702–9707. https://doi.org/10.1016/j.jpowsour.2011.07.054.

[19] Q.Y. Wang, J. Liu, A.V. Murugan, A. Manthiram, High capacity double-layer surface modified

$Li[Li_{0.2}Mn_{0.54}Ni_{0.13}Co_{0.13}]O_2$ cathode with improved rate capability, J. Mater.Chem. 19 (2009) 4965–4972. https://doi.org/10.1039/B823506F.

[20] J. Gao, J. Kim, A. Manthiram, High capacity $Li[Li_{0.2}Mn_{0.54}Ni_{0.13}Co_{0.13}]O_2$–$V_2O_5$ composite cathodes with low irreversible capacity loss for lithium ion batteries, Electrochem. Commun. 11 (2009) 84–86. https://doi.org/10.1016/j.elecom.2008.10.036.